

Received August 14, 2014; reviewed; accepted October 1, 2014

## HYDROXYAPATITE AS A SUPPORT IN PROTEASE IMMOBILIZATION PROCESS

Jakub ZDARTA<sup>\*</sup>, Katarzyna BUDZINSKA<sup>\*</sup>, Agnieszka KOLODZIEJCZAK-  
RADZIMSKA<sup>\*</sup>, Lukasz KLAPISZEWSKI<sup>\*</sup>, Katarzyna SIWINSKA-  
STEFANSKA<sup>\*</sup>, Przemyslaw BARTCZAK<sup>\*</sup>, Adam PIASECKI<sup>\*\*</sup>,  
Hieronim MACIEJEWSKI<sup>\*\*\*,\*\*\*\*</sup>, Teofil JESIONOWSKI<sup>\*</sup>

<sup>\*</sup> Poznan University of Technology, Faculty of Chemical Technology, Institute of Chemical Technology and Engineering, Berdychowo 4, PL-60965, Poznan, Poland, teofil.jesionowski@put.poznan.pl

<sup>\*\*</sup> Poznan University of Technology, Faculty of Mechanical Engineering and Management, Institute of Materials Science and Engineering, Jana Pawla II 24, PL-60965, Poznan, Poland

<sup>\*\*\*</sup> Adam Mickiewicz University in Poznan, Faculty of Chemistry, Umultowska 89b, PL-61614 Poznan, Poland

<sup>\*\*\*\*</sup> Poznan Science and Technology Park, A. Mickiewicz University Foundation, Rubiez 46, Poznan, Poland

**Abstract:** Hydroxyapatite is used as a matrix for immobilization of protease from *Aspergillus oryzae* by a process of adsorption. The matrix obtained has the surface area of 26 m<sup>2</sup>/g and particles in the shape of flakes of diameters no greater than 650 nm. The efficiency of the proposed method was confirmed by the Fourier transform infrared spectroscopy, elemental analysis and by analysis of parameters of the pore structure of matrix and products after immobilization. On the basis of the Bradford method it was found that the greatest amount of enzyme (132 mg/g) was immobilized from a solution of initial enzyme concentration of 7 mg/cm<sup>3</sup> after 24 h of the process.

**Keywords:** hydroxyapatite, enzyme immobilization, protease, physicochemical characteristic

### Introduction

Proteases (also termed peptidases) make a well-known group of enzymes responsible for division of long chains of amino acids into shorter fragments through a process of hydrolysis of peptide bonds. The biocatalysts are characterized by high activity in a wide range of temperatures (30-80 °C) and pH (5-10), with the maximum activity at 40 °C and at pH 8 (Li et al., 2011). Enzymes from this group are produced by many micro-organisms such as bacteria, yeast, fungi, but their industrial production is based on the use of two fungi species from families of *Aspergillus* and *Bacillus* (Sharma et al., 2013). Peptidases have been applied in pharmaceutical industry, leather industry as

well as in production of food and detergents (Sarker et al., 2013). They have been also added to fodder (Dragomirescu et al., 2012). Recently, they have been increasingly used for bioremediation of water and sewage (Padmapriya et al., 2012). Similar use have ureases, enzymes of a hydrolase class, that are used in wastewater treatment (Krajewska 2009 a, b). A very good support for this group of enzymes is hydroxyapatite (HA) ( $\text{Ca}_{10}(\text{PO}_4)_6(\text{OH})_2$ ) (Jesionowski et al., 2014), which is inorganic and water insoluble mineral belonging to the family of calcium phosphates. The most important advantages of HA are biocompatibility, bioactivity, non-toxicity and immunogenic properties (Pahm et al., 2013). The application of hydroxyapatite is limited because of its low mechanical strength (Liu et al., 2014).

In nature, hydroxyapatite (HA) occurs as mineral and it also makes about 80% wt. of bones (Daniels et al., 2010, Xing et al., 2014). Because of its properties, hydroxyapatite is a very good substitute of bones and has been of great interest in tissue engineering (Alves Cardoso et al., 2012). In pharmaceuticals it has been used as a support of drugs (Zhang et al., 2012), and after introduction of titanium ions into its structure, it has been used for decomposition of pathogens in a blood purification therapy upon UV irradiation (Kandori et al., 2013). Hydroxyapatite is also able to bind metal ions from water solutions, especially if it is a component of composite materials. Thus, hydroxyapatite is applied for removal of toxic metal ions from wastewater and soil (Carro et al., 2013). HA has been also proved, to be an effective adsorbent of lead ions (Ramesh et al., 2013, Cui et al., 2013), and when modified with lead ions, it shows high ability to remove uranium ions (Popa 2013). Besides the application in medicine and for remediation of natural environment, hydroxyapatite is also used in electrochemistry for production of biological sensors (Ma et al., 2009). Another application of hydroxyapatite is in packing of chromatographic columns used for separation of proteins, enzymes or DNA (Dancu et al., 2011).

This study was undertaken to check a possibility of using hydroxyapatite as a support for enzyme immobilization. The method proposed permits stabilization of enzyme structure and improvement in its properties (Rodrigues et al., 2013).

Salman et al. (2008) used the HA matrix for multiple enzyme immobilization in biodetectors for calorimetric evaluation of glucose and urea content. The results proved that the method and established parameters of reaction are suitable for the regular analysis of reversible adsorption *in situ*, for the same biosensors. An attempt was also made to immobilize the recombined human morphogenetic bone protein (rhBMP-2) on the surface of unmodified and modified hydroxyapatite. Adsorption of the protein growth agent was confirmed. These data may be used as the basis for formulation of theoretical description for delivery of drugs that increase the rate of bone growth and osteointegration of implants (Zurlinden et al., 2005). Hydroxyapatite was also tested for applications in encapsulation of alkaline phosphatase. The analysis of results confirmed immobilization of enzyme and preservation of the biocatalyst activity. This protein takes part in mineralization of new bones as they form. Thus, an attempt was made to evaluate the efficiency of substance obtained during the process

of stimulated bone formation (Jiang et al., 2010). The subject of other papers involved the binding of fusion protein FN<sub>RGD</sub>/OC onto the surface of hydroxyapatite. The results illustrated the advantage of immobilized FN<sub>RGD</sub>/OC over the native FN, which manifested as intensification in osteoblasts proliferation. Therefore, the strategy for designing multifunctional proteins integrated into the hydroxyapatite matrix can be used for bone regeneration (Kang et al., 2011). During immobilization, it is important to ensure the possibility of repeated use of enzyme. The method of repeatable adsorption and total removal of protein from the hydroxyapatite surface has been presented. The ability to reuse the HA support for adsorption of fibrinogen and FBS proteins has been proved (Tagaya et al., 2010).

The hitherto results have brought a substantial contribution to dynamic development of immobilization of enzymes on the surface of hydroxyapatite. However, there are still many problems that need detailed solutions, which have prompted us to undertake the study reported in this work. The aim of our study was immobilization of *Aspergillus oryzae* protease by adsorption on the surface of hydroxyapatite. A comprehensive physicochemical analysis of the support was made and the effectiveness of proposed procedure of enzyme immobilization was evaluated. The amount of adsorbed protein and changes in the content of particular elements in the products after immobilization were established. The changes in the porous structure of the support after immobilization additionally confirmed the process efficiency.

## Experimental

### Materials

Ethyl alcohol (purity 96%), phosphoric acid (purity 85%) and calcium chloride were purchased from Chempur Company (Poland). Phosphate buffer of pH=7 was obtained from Amresco Company (USA). Protease (PRT) from *Aspergillus oryzae*, sodium phosphate dibasic and Coomassie Brilliant Blue were purchased from Sigma–Aldrich (Germany).

### Preparation of hydroxyapatite

The procedure for obtaining hydroxyapatite was as follows. A proper volume of 1 M calcium chloride solution was placed in a reactor equipped with a high-speed stirrer (ca. 900 rpm) mounted in a water bath of 40 °C. To the reactor a 100 cm<sup>3</sup> of 0.6 M sodium phosphate dibasic solution dissolved in ethyl alcohol was dosed. Then, the mixture was stirred for about 15 min, filtered off under reduced pressure on a Sartorius AG set (Germany) and washed with water. A scheme of HA preparation is shown in Fig. 1. The product was dried at 120 °C in a Memmert dryer (Germany) and subjected to calcination at 600 °C in a Nabertherm furnace (Germany). Finally, obtained hydroxyapatite was ground and sieved through sieve of 63 μm.

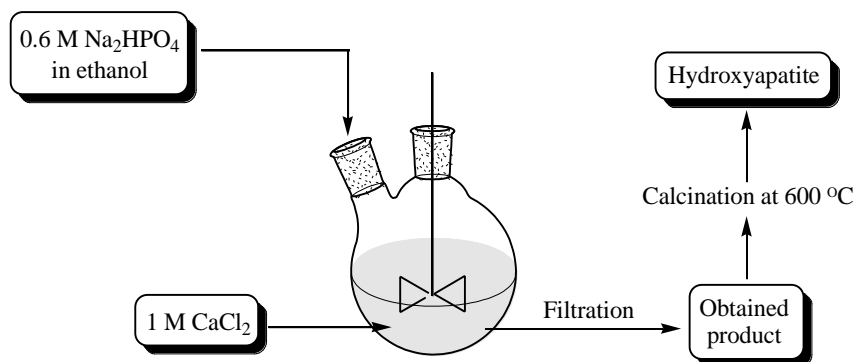


Fig. 1. Schematic diagram of hydroxyapatite preparation

### Immobilization of protease onto hydroxyapatite surface

To each of three conical flasks a portion of 500 mg hydroxyapatite was introduced and then 15 cm<sup>3</sup> of the enzyme solution with concentrations of 3, 5 and 7 mg/cm<sup>3</sup> at phosphate buffer of pH=7 was added. The process of immobilization was performed in different times, from 1 min to 96 h, at ambient temperature. After completion of the process, the mixtures were filtered off under reduced pressure and the obtained products were dried in air at room temperature for 24 h.

### Evaluation of physicochemical properties

The dispersive characteristics of hydroxyapatite were determined using a Zetasizer Nano ZS apparatus made by Malvern Instruments Ltd. (UK), operating on the non-invasive back-scattering method and measuring particles with sizes between 0.6 to 6000 nm.

On the basis of SEM image recorded by an EVO40 scanning electron microscope (Zeiss, Germany), the surface morphology and microstructure of hydroxyapatite was examined.

Fourier transform infrared spectroscopy (FTIR), recorded by an Vertex 70 spectrometer (Bruker, Germany) was used to obtain the presence of functional groups. The investigation was performed at a resolution of 0.5 cm<sup>-1</sup>.

The elemental contents of carbon, hydrogen and nitrogen were established by using a Vario EL Cube instrument made by Elementar Analysensysteme GmbH (Germany)

The surface composition of hydroxyapatite (contents of Ca and P) was analysed by energy dispersive X-ray spectroscopy (EDX) using a Princeton Gamma-Tech unit equipped with a prism digital spectrometer (Germany). EDX technique is based on analysis of X-ray energy values using a semiconductor. Before the analysis, samples were placed on a special carbon tape. The presence of carbon materials is needed to create a conductive layer which ensures delivery of electric charge from the sample. Representative parts (500 μm<sup>2</sup>) were analyzed for proper evaluation of surface composition.

Hydroxyapatite was also subjected to crystalline structure determination using the WAXS method (wide-angle X-ray scattering). X-ray diffraction measurements were performed using  $\text{CuK}_\alpha$  ( $\lambda = 0.15418$  nm) radiation. The accelerating voltage and applied current were 30 kV and 25 mA, respectively. The other measurement parameters were as follows:  $2\theta$  angle range  $5\text{--}60^\circ$ , counting step ( $2\theta$ )  $0.04^\circ$ , counting time 3 s.

In order to characterize the porous structure of the examined substances, their surface area, pore volume and average pore size were determined using an ASAP 2020 instrument, Micromeritics Instrument Co. (USA). All samples were degassed at  $120^\circ\text{C}$  for 4 h in a vacuum chamber prior to measurement. The surface area was determined by the multipoint Brunauer–Emmett–Teller (BET) method (Sing et al., 1985, Foo et al., 2010). The Barrett–Joyner–Halenda (BJH) method was applied to determine the pore volume and average pore size (Barrett et al., 1951).

The amount of enzyme adsorbed and immobilization yield was determined according to the Bradford method using bovine serum albumin as a standard (Bradford, 1976). Spectrophotometric measurements needed for the calculations were made by using a UV-1601 PC Shimadzu spectrophotometer (Japan) at 595 nm. Prior to measurements, a reagent composed of Coomassie Brilliant Blue G-250, 85% phosphoric acid and 96% ethyl alcohol was made and added to the albumin solution. It was also used as a reference substance.

During evaluation of efficiency of the process, the amount of enzyme adsorbed per a time unit  $q_t$  was determined using the formula:

$$q_t = \frac{(C_0 - C_t) \cdot V}{m} \quad (1)$$

where  $C_0$  and  $C_t$  denote concentrations of enzyme ( $\text{mg}/\text{cm}^3$ ) in the solution before and after adsorption, respectively;  $V$  is volume of solution ( $\text{cm}^3$ ), and  $m$  is the mass of the hydroxyapatite support (g).

## Results and discussion

### Hydroxyapatite characterization

Morphology of obtained hydroxyapatite was characterized using scanning electron microscope images presented in Fig. 2. The SEM images show that hydroxyapatite particles are in the form of flakes, which tend to form aggregates. Hydroxyapatite characterized in earlier works (Bardhan, 2011) had similar morphology. To supplement the data from SEM, the particle size distribution was determined and the obtained results are presented in Fig. 3. Figure 3 shows that obtained hydroxyapatite has a monomodal particle size distribution in the range of 396–615 nm, corresponding to primary particles showing a tendency to aggregate. Over 70% of the volume

contribution is taken by the particles of 531 nm (39.3%) and 459 nm (35.7%). The particle size distribution is in agreement with that reported by Earl *et al.* (2006).

At the next step the crystalline structure of hydroxyapatite obtained was resolved. It was shown that the proposed in this work procedure leads to formation of crystalline hydroxyapatite, which is confirmed by the presence of diffraction maxima for  $2\theta$  of 26, 32, 33, 34, 40, 47, 49 and 54 in the X-ray diffractogram (Fig. 4) (Kolodziejczak-Radzimska *et al.*, 2014). To confirm the presence of elemental characteristic of hydroxyapatite, the EDX analysis as well as the elemental analysis were made. According to the results, the content of calcium in the obtained material is higher than that of phosphorus and the mass ratio of Ca/P is close to 1.5. Based on elemental analysis, the presence of carbon and hydrogen was noted as 22% of C and 1.07% of H).

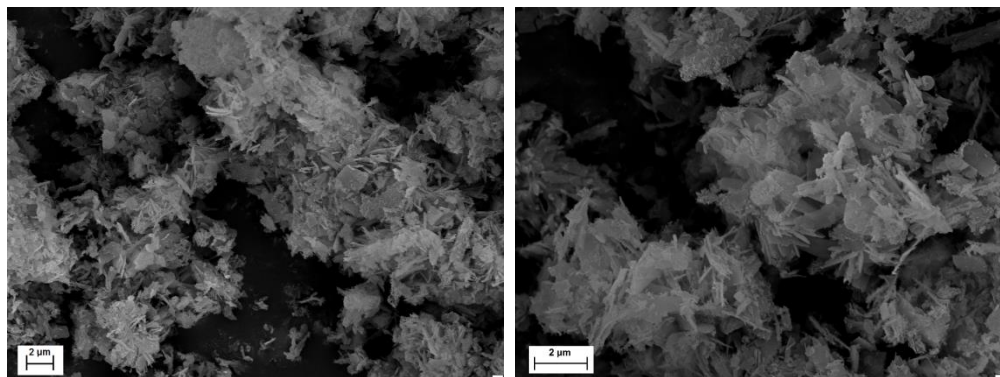


Fig. 2. SEM images of obtained hydroxyapatite (at different magnifications)

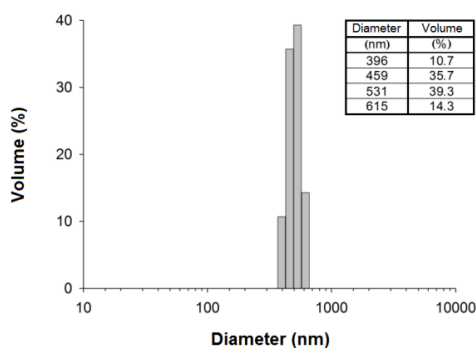


Fig. 3. Particle size distribution of obtained hydroxyapatite support

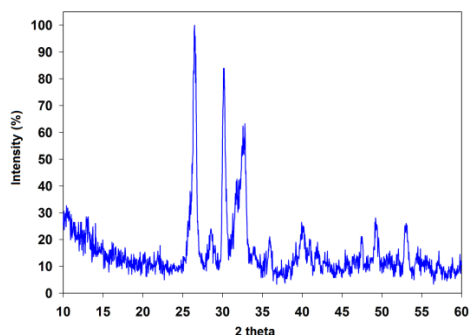


Fig. 4. XRD pattern of hydroxyapatite support

### Characterization of products after protease immobilization

To verify enzyme immobilization on the hydroxyapatite surface, the FTIR spectra of samples were recorded and analyzed. Figure 5 presents results of spectroscopic study of hydroxyapatite and products after 24 h of immobilization from the solutions with different concentrations. The most important fragment of the spectra, from 1700 to 1200  $\text{cm}^{-1}$ , was magnified. The spectrum of hydroxyapatite shows a broad signal between wavenumbers 3550 and 3200  $\text{cm}^{-1}$  generated by the stretching vibrations of hydroxyl groups, while the signal with the maximum at 1630  $\text{cm}^{-1}$  is assigned to physically adsorbed water. The bands at 1200, 1050 and 600  $\text{cm}^{-1}$ , a very characteristic of hydroxyapatite, are assigned to the stretching vibrations of phosphate groups ( $\text{PO}_4^{3-}$ ) (Uddin, 2010). The band at 800  $\text{cm}^{-1}$  is assigned to the hydrophosphate ions ( $\text{HPO}_4^{2-}$ ) (Uddin, 2010).

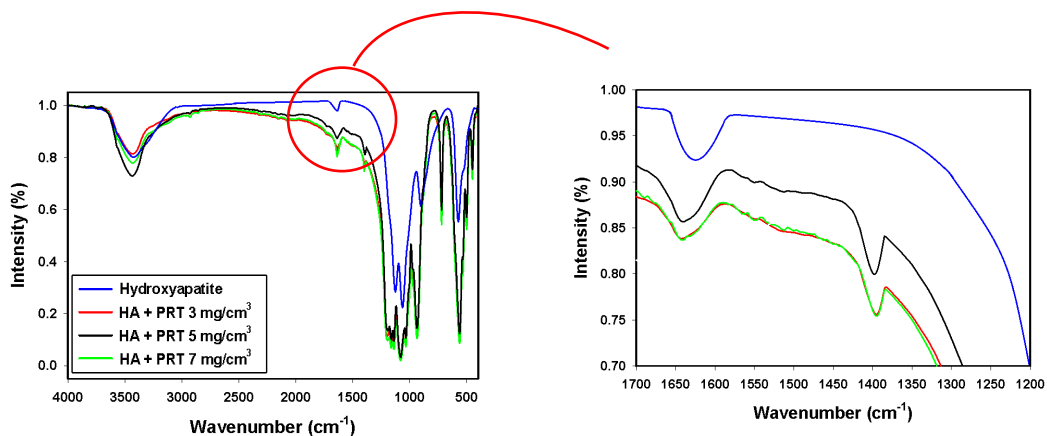


Fig. 5. FTIR spectra of hydroxyapatite and products after protease immobilization for 24 h from enzyme solution with various concentration

The characteristic bands of protease appear at the wavenumber of  $2900\text{ cm}^{-1}$ , and in the range of  $1700\text{--}1200\text{ cm}^{-1}$ . Their presence confirms immobilization of protease on the support. The band about  $2900\text{ cm}^{-1}$  is assigned to the stretching vibrations of methyl and methylene groups ( $-\text{CH}_2$  and  $-\text{CH}_3$ ). The signal at about  $1650\text{ cm}^{-1}$  corresponds to the stretching vibrations of  $\text{C}=\text{C}$  bonds (Ozsagiroglu, 2012). The band at about  $1400\text{ cm}^{-1}$  is generated by the vibrations of  $-\text{C}-\text{N}$  bonds in the protease molecule (Singh, 2011). The FTIR spectra after immobilization of the biocatalyst also show the signals at  $700\text{ cm}^{-1}$  and  $490\text{ cm}^{-1}$ , and their presence is assigned to the wagging vibrations and out-of-plane vibrations of  $\text{C}-\text{H}$  bonds in protease (Zhang, 2006). Moreover, the spectra show the bands at the same wavenumbers, at which the hydroxyapatite bands occur but of higher intensity than in the spectra of hydroxyapatite. It is a result of the presence of  $-\text{C}-\text{O}$  bonds in the protease molecule, which vibrations are manifested as the signals at  $1150\text{ cm}^{-1}$  and  $1050\text{ cm}^{-1}$ . A similar situation takes place for the signals assigned to the vibrations of hydroxyl groups, they also become more intense after immobilization.

The spectrophotometric analysis performed on the basis of the Bradford method (Bradford, 1976), permits estimation of the amount of enzyme adsorbed on the support surface per 1 g of the matrix. The relevant data are presented in Table 1.

Table 1. Amount of immobilized enzyme

Immobilization time	Enzyme concentration ( $\text{mg}/\text{cm}^3$ )		
	3	5	7
Amount of immobilized enzyme ( $\text{mg}/\text{g}$ )			
1 (min)	52	70	76
5 (min)	53	73	96
10 (min)	58	75	108
30 (min)	59	78	115
60 (min)	60	80	118
120 (min)	63	82	123
24 (h)	67	91	132
96 (h)	68	91	132

The analysis of the data from Table 1 shows that with increasing initial concentration of enzyme in solution, the amount of protease immobilized on the hydroxyapatite matrix increases. The greatest amount of protease (132 mg) per gram of the matrix was immobilized from the protease solution of  $7\text{ mg}/\text{cm}^3$  after 24 h of the process. Immobilization is the most effective in the first minutes of the adsorption process. The rate of adsorption decreases with time and after 24 h the increase in the mass of protease is no longer detectable. The time of 24 h was found to be the optimum for immobilization by adsorption of protease onto the hydroxyapatite surface. Based on the increase of amount of immobilized enzyme, which raises with



raise of initial concentration of peptide solution, curves presenting dependence of  $q_t$  on time were evaluated (Fig. 6).

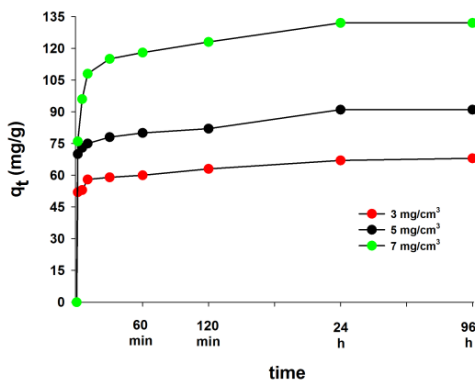


Fig. 6. Effect of contact time on enzyme adsorbed by HA (enzyme concentration 3, 5 and 7 mg/cm<sup>3</sup>, HA dose 0.5 g)

Figure 6 shows a plot of the amount of enzyme adsorbed (mg/g) versus contact time for different initial enzyme concentrations of 1, 5 and 7 mg/cm<sup>3</sup>. Noteworthy, for each model concentration of enzyme in solution (3-7 mg/cm<sup>3</sup>) the adsorption equilibrium is reached after 24 h. The equilibrium concentration ( $q_e$ ) was equal to 68, 91, 132 mg/g for 1, 5 and 7 mg/cm<sup>3</sup>, respectively.

Based on the data from Table 1, the effectiveness of proposed method was calculated and the results are presented in Table 2. The immobilization yield (%) was calculated basing on the following equation:

$$I_y = \frac{A_I \cdot 100\%}{A_T} \quad (2)$$

where  $I_y$  is immobilization yield (%),  $A_I$  amount of immobilized enzyme and  $A_T$  is amount of immobilized enzyme with 100% yield.

Tables 1 and 2 show that the yield of the process is not correlated with the amount of immobilized enzyme. The highest yield of 75.6 % was obtained for adsorption from the initial enzyme solution of concentration 3 mg/cm<sup>3</sup> for the reaction time of 96 h. The lowest yield of about 60% was obtained for the process performed from the initial enzyme concentration of 5 mg/cm<sup>3</sup>. It should be noted that for each initial enzyme concentration the yield after one minute of the process is higher than half of its maximum value, what means that over half of the enzyme amount gets immobilized at the beginning of the process. This observation can be explained by the fact that most of the active sites of the hydroxyapatite matrix saturated at the beginning of adsorption because of a high concentration of protease in the initial solutions.

Table 2. Protease immobilization yield

Immobilization time	Enzyme concentration (mg/cm <sup>3</sup> )		
	3	5	7
	Immobilization yield (%)		
1 (min)	57.8	46.7	36.2
5 (min)	58.9	48.7	45.7
10 (min)	64.4	50.0	51.4
30 (min)	65.6	52.0	54.8
60 (min)	66.7	53.3	56.2
120 (min)	70.0	54.7	58.6
24 (h)	74.4	60.7	62.9
96 (h)	75.6	60.8	63.0

Effective immobilization of protease on the surface of hydroxyapatite is also confirmed by the results of elemental analysis. The results revealed changes in the contents of the most important elements (N, C, H) in the samples after immobilization. The changes dependent on time of adsorption and concentration of enzyme solution. The results are shown in Table 3. The hydroxyapatite used contained 1.07% of hydrogen and 0.22% of carbon. After enzyme immobilization, the samples revealed increase in contents of hydrogen and carbon, but also in content of nitrogen coming from enzyme (Xiaochun, 2013). The elemental analysis showed the increase in the content of C, H, N elements in the samples after immobilization, irrespective of adsorption time. The most pronounced changes were noted in the content of carbon. In the samples after immobilization lasting for 96 h from the solution of initial concentration of 7 mg/cm<sup>3</sup>, the content of carbon increased over twice with respect to

Table 3. Results of elemental analysis for hydroxyapatite matrix and products

Enzyme concentration (mg/cm <sup>3</sup> )	Immobilization time	Elemental analysis (%)		
		N	C	H
Hydroxyapatite (HA)		-	0.22	1.07
3	60 (min)	0.10	0.32	1.13
	24 (h)	0.11	0.33	1.14
	96 (h)	0.11	0.34	1.14
5	60 (min)	0.10	0.37	1.14
	24 (h)	0.12	0.38	1.15
	96 (h)	0.12	0.39	1.15
7	60 (min)	0.12	0.41	1.16
	24 (h)	0.13	0.44	1.19
	96 (h)	0.13	0.44	1.19

that in the hydroxyapatite matrix. The increase in the content of hydrogen and nitrogen was not so great, but with increasing the initial enzyme concentration and time of immobilization process, the percentage contribution of these elements in the samples increased.

In the next step, the parameters of porous structure of hydroxyapatite matrix and samples after immobilization were determined to analyse the effect of immobilization on the surface area, pore size and pore volume. The results for selected times of immobilization are presented in Table 4. Hydroxyapatite has BET surface area of 26 m<sup>2</sup>/g, which decreases as a result of immobilization. The changes are most pronounced in the samples obtained after adsorption lasting 96 h, irrespective of the enzyme concentration in the initial solution. The smallest surface area was determined for the sample after immobilization from the solution of the highest concentration. Similar tendencies were observed for the pore size and total pore volume. The hydroxyapatite matrix contained pores of 2.7 nm in diameter (on average) and total volume of 0.018 cm<sup>3</sup>/g. The changes in the porous structure observed after the process of immobilization, i.e. decreased surface area, average pore diameter and total pore volume, evidence the effectiveness of the process (Gustafsson et al., 2012). With increasing time of the process and initial concentration of enzyme solution, a significant decrease in the values of above mentioned parameters was observed (Table 4). The smallest average pore diameter and total pore volume were found in the sample after immobilization of protease for 96 h from the enzyme solution of initial concentration 7 mg/cm<sup>3</sup> (pore size 1.3 nm and pore volume 0.005 cm<sup>3</sup>/g). It should be added that the results obtained for the samples after immobilization lasting for 24 h and 96 h did not differ much, what suggests on small changes in the hydroxyapatite structure taking place after 24 h of immobilization.

Table 4. Porous structure parameters of obtained HA and products after immobilization

Enzyme concentration (mg/cm <sup>3</sup> )	Immobilization time	BET surface area (m <sup>2</sup> /g)	Pore volume (cm <sup>3</sup> /g)	Pore size (nm)
Hydroxyapatite (HA)		26	0.018	2.7
3	60 (min)	17	0.011	2.1
	24 (h)	15	0.009	1.7
	96 (h)	15	0.008	1.7
5	60 (min)	15	0.010	1.7
	24 (h)	13	0.007	1.5
	96 (h)	13	0.006	1.5
7	60 (min)	14	0.008	1.5
	24 (h)	12	0.005	1.3
	96 (h)	11	0.005	1.3

## Conclusions

The proposed in this work method for synthesis of hydroxyapatite gave a product made of particles in the shape of flakes of sizes not exceeding 650 nm. The obtained matrix had well-developed crystalline structure characteristic of hydroxyapatite and the Ca/P mass ratio of about 1.5. The obtained data showed that the method proposed for immobilization of protease is effective and leads to immobilization of enzyme on the matrix surface. The evidence of successful immobilization was provided by the FTIR study, Bradford method measurements, elemental analysis and character of porous structure of products after immobilization, with respect to those of the initial matrix. The process of immobilization on the hydroxyapatite surface was performed for different times, where the optimum duration was 24 h since after this time no significant increase in the amount of enzyme was noted. The greatest amount of enzyme (132 mg/g) was immobilized from the solution of initial concentration of 7 mg/cm<sup>3</sup>, however, the highest yield of the process (over 75%) was obtained from the solution of initial enzyme concentration of 3 mg/cm<sup>3</sup>.

## Acknowledgements

This work was supported by the Poznan University of Technology research grant no. 03-32-443/2014-DS-PB.

## References

- ALVES CARDOSO D., JANSEN J.A., LEEUWENBURGH S.C.G., 2012, *Synthesis and application of nanostructured calcium phosphate ceramics for bone regeneration*, Journal of Biomedical Materials Research B: Applied Biomaterials, 100, 2316–2326.
- BARDHAN R., MAHATA S., MONDAL B., 2011, *Processing of natural resourced hydroxyapatite from eggshell waste by wet precipitation method*, Advances in Applied Ceramics, 110, 80–86.
- BARRETT E.P., JOYNER L.G., HALENDA P.H., 1951, *The determination of pore volume and area distributions in porous substances. I. Computations from nitrogen isotherms*, Journal of the American Chemical Society, 73, 373–380.
- BRADFORD M.M., 1976, *A rapid and sensitive method for the quantitation of microgram quantities of protein utilizing the principle of protein-dye binding*, Analytical Biochemistry, 72, 248–254.
- CARRO L., HABLOT E., CORADIN T., 2013, *Hybrids and biohybrids as green materials for a blue planet*, Journal of Sol-Gel Science and Technology, 70, 263–271.
- CUI H., ZHOU J., ZHAO Q., SI Y., MAO J., FANG G., LIANG J., 2013, *Fractions of Cu, Cd, and enzyme activities in a contaminated soil as affected by applications of micro- and nanohydroxyapatite*, Journal of Soils and Sediments, 13, 742–752.
- DANCU A.-C., BARABAS R., BOGYA E.-S., 2011, *Adsorption of nicotinic acid on the surface of nanosized hydroxyapatite and structurally modified hydroxyapatite*, Central European Journal of Chemistry, 9, 660–669.
- DANIELS Y., ALEXANDRATOS S.D., 2010, *Design and synthesis of hydroxyapatite with organic modifiers for application to environmental remediation*, Waste Biomass Valor, 1, 157–162.

- DRAGOMIRESCU M., PREDA G., VINTILA T., VLAD-OROS B., BORDEAN D., SAVII C., 2012, *The effect of immobilization on activity and stability of a protease preparation obtained by an indigenous strain, Bacillus licheniformis B 40*, Revue Roumaine de Chimie, 57, 77–84.
- EARL J.S., WOOD D.J., MILNE S.J., 2006, *Hydrothermal synthesis of hydroxyapatite*, Journal of Physics: Conference Series, 26, 268–271.
- FOO K.Y., HAMEED B.H., 2010, *Insights into the modeling of adsorption isotherm systems*, Chemical Engineering Journal, 156, 2–10.
- GUSTAFSSON H., JOHANSSON E., BARRABINO A., ODEN M., HOLMBERG K., 2012, *Immobilization of lipase from Mucor miehei and Rhizopus oryzae into mesoporous silica*, Colloids and Surfaces B: Biointerfaces, 100, 22–30.
- JIANG P.J., WYNN-JONES G., GROVER L.M., 2010, *A calcium phosphate cryogel for alkaline phosphatase encapsulation*, Journal of Materials Science, 45, 5257–5263.
- JESIONOWSKI T., ZDARTA J., KRAJEWSKA B., 2014, *Enzymes immobilization by adsorption: A review*, Adsorption, 20, 801–821.
- KANDORI K., OKETANI M., WAKAMURA M., 2013, *Effects of Ti(IV) substitution on protein adsorption behaviors of calcium hydroxyapatite particles*, Colloids and Surfaces B: Biointerfaces, 101, 38–73.
- KANG W., KIM T.-I., YUN Y., KIM H.-W., JANG J.-H., 2011, *Engineering of a multi-functional extracellular matrix protein for immobilization to bone mineral hydroxyapatite*, Biotechnology Letters, 33, 199–204.
- KOLODZIEJCZAK-RADZIMSKA A., SAMUEL M., PAUKSZTA D., PIASECKI A., JESIONOWSKI T., 2014, *Synthesis of hydroxyapatite in the presence of anionic surfactant*, Physicochemical Problems of Mineral Processing 50, 225–236.
- KRAJEWSKA, B., 2009 a, *Ureases I. Functional, catalytic and kinetic properties: A review*, Journal of Molecular Catalysis B: Enzymatic 56, 9–21.
- KRAJEWSKA, B., 2009 b, *Ureases. II. Properties and their customizing by enzyme immobilizations: A review*, Journal of Molecular Catalysis B: Enzymatic 59, 22–40.
- LI G.Y., CAI Y.J., LIAO X.R., YIN J., 2011, *A novel nonionic surfactant- and solvent-stable alkaline serine protease from Serratia sp. SYBC H with duckweed as nitrogen source: Production, purification, characteristics and applications*, Journal of Industrial Microbiology and Biotechnology, 38, 845–853.
- LIU Y., HUANG J., LI H., 2014, *Nanostructural characteristics of vacuum cold-sprayed hydroxyapatite /graphene-nanosheet coatings for biomedical applications*, Journal of Thermal Spray Technology, 23(7), 1149–1156.
- MA R., WANG B., LIU Y., LI J., ZHAO Q., WANG G., JIA W., WANG H., 2009, *Direct electrochemistry of glucose oxidase on the hydroxyapatite/Nafion composite film modified electrode and its application for glucose biosensing*, Science in China Series B: Chemistry, 52, 2013–2019.
- OZSAGIROGLU E., IYISAN B., GUVENILIR Y.A., 2012, *Biodegradation and characterization studies of different kinds of polyurethanes with several enzyme solutions*, Polish Journal of Environmental Studies, 21, 1777–1782.
- PADMAPRIYA M., WILLIAMS B.C., 2012, *Purification and characterization of neutral protease enzyme from Bacillus subtilis*, Journal of Microbiology and Biotechnology Research, 2, 612–618.
- PHAM T.T.T., NGUYEN T.P., PHAM T.N., VU T.P., TRAN D.L., TAHI H., DINH T.M.T., 2013, *Impact of physical and chemical parameters on the hydroxyapatite nanopowder synthesized by chemical precipitation method*, Advances in Natural Sciences: Nanoscience and Nanotechnology, 4, 1–9.

- POPA K., 2013, *Sorption of uranium on lead hydroxyapatite*, Journal of Radioanalytical and Nuclear Chemistry, 298, 1527–1532.
- RAMESH S.T., RAMESHBABU N., GANDHIMATHI R., KUMAR M.S., NIDHEESH P.V., 2013, *Adsorptive removal of Pb(II) from aqueous solution using nano-sized hydroxyapatite*, Applied Water Science, 3, 105–113.
- RODRIGUES R.C., ORTIZ C., BERENQUER-MURCIA A., TORRES R., FERNANDEZ-LAFUENTE R., 2013, *Modifying enzyme activity and selectivity by immobilization*, Chemical Society Reviews, 42, 6290–6307.
- SALMAN S., SOUNDARARAJAN S., SAFINA G., SATOH I., DANIELSSON B., 2008, *Hydroxyapatite as a novel reversible in situ adsorption matrix for enzyme thermistor-based FIA*, Talanta, 77, 490–493.
- SARKER P.K., TALUKDAR S.A., DEB P., SAYEM S.M.A., MOHSINA K., 2013, *Optimization and partial characterization of culture conditions for the production of alkaline protease from Bacillus licheniformis P003*, Springer Plus, 2, 506–517.
- SHARMA N., TRIPATHI S., 2013, *Kinetic study of free and immobilized protease from Aspergillus sp.*, Journal of Pharmacy and Biological Sciences, 7, 86–96.
- SING K.S.W., EVERETT D.H., HAUL R.A.W., MOSCOU L., PIEROTTI R.A., ROUQUEROL J., SIEMIENIEWSKA T., 1985, *Reporting physisorption data for gas/solid systems with special reference to the determination of surface area and porosity*, Pure and Applied Chemistry, 57, 603–619.
- SINGH A.N., SINGH S., SUTHAR N., DUBEY V.K., 2011, *Glutaraldehyde-activated chitosan matrix for immobilization of a novel cysteine protease*, Procerain B, Journal of Agricultural and Food Chemistry, 59, 6256–6262.
- TAGAYA M., IKOMA T., HANAGATA N., CHAKAROV D., KASEMO B., TANAKA J., 2010, *Reusable hydroxyapatite nanocrystal sensors for protein adsorption*, Science and Technology of Advanced Materials, 11, 1–8.
- UDDIN M.H., MATSUMOTO T., ISHIHARA A., OKAZAKI M., SOHUMURA T., 2010, *Apatite containing aspartic for selective protein loading*, Journal of Dental Research, 89, 488–492.
- XIAOCHUN L., SHANGYU D., CHUANGYE Y., XINGI G., JIAWEI W., YIGONG S., 2013, *Structure of a presenilin family intramembrane aspartate protease*, Nature, 493, 56–61.
- XING Z.-C., CHANG H.-W., CHUN S., KIM S., KANG I.-K., 2014, *Immobilization of collagen on hydroxyapatite discs by covalent bonding and physical adsorption and their interaction with MC3T3-E1 osteoblasts*, Tissue Engineering and Regenerative Medicine, 11, 1–7.
- ZHANG L.-X., WANG J., WEN J.-Q., LIANG H.-G., DU L.-F., 2006, *Purification and partial characterization of a protease associated with photosystem II particles*, Physiologia Plantarum, 95, 591–595.
- ZHANG X., ZHANG W., YANG Z., ZHANG Z., 2012, *Nanostructured hollow spheres of hydroxyapatite: preparation and potential application in drug delivery*, Frontiers of Chemical Science and Engineering, 6, 246–252.
- ZURLINDEN K., LAUB M., JENNISSEN H.P., 2005, *Chemical functionalization of a hydroxyapatite based bone replacement material for the immobilization of proteins*, Materialwissenschaft und Werkstofftechnik, 36, 820–827.